

Antimicrobial Effects of Interferon-Inducible CXC Chemokines against *Bacillus anthracis* Spores and Bacilli[∇]

Matthew A. Crawford,¹ Yinghua Zhu,¹ Candace S. Green,¹ Marie D. Burdick,² Patrick Sanz,³ Farhang Alem,³ Alison D. O'Brien,³ Borna Mehrad,² Robert M. Strieter,² and Molly A. Hughes^{1*}

Department of Medicine, Division of Infectious Diseases, University of Virginia Health Sciences System, Charlottesville, Virginia¹;
Department of Medicine, Division of Pulmonary and Critical Care Medicine, University of Virginia Health Sciences System, Charlottesville, Virginia²; and Department of Microbiology and Immunology, Uniformed Services University of the Health Sciences, Bethesda, Maryland³

Received 29 September 2008/Returned for modification 10 November 2008/Accepted 21 January 2009

Based on previous studies showing that host chemokines exert antimicrobial activities against bacteria, we sought to determine whether the interferon-inducible Glu-Leu-Arg-negative CXC chemokines CXCL9, CXCL10, and CXCL11 exhibit antimicrobial activities against *Bacillus anthracis*. In vitro analysis demonstrated that all three CXC chemokines exerted direct antimicrobial effects against *B. anthracis* spores and bacilli including marked reductions in spore and bacillus viability as determined using a fluorometric assay of bacterial viability and CFU determinations. Electron microscopy studies revealed that CXCL10-treated spores failed to undergo germination as judged by an absence of cytological changes in spore structure that occur during the process of germination. Immunogold labeling of CXCL10-treated spores demonstrated that the chemokine was located internal to the exosporium in association primarily with the spore coat and its interface with the cortex. To begin examining the potential biological relevance of chemokine-mediated antimicrobial activity, we used a murine model of inhalational anthrax. Upon spore challenge, the lungs of C57BL/6 mice (resistant to inhalational *B. anthracis* infection) had significantly higher levels of CXCL9, CXCL10, and CXCL11 than did the lungs of A/J mice (highly susceptible to infection). Increased CXC chemokine levels were associated with significantly reduced levels of spore germination within the lungs as determined by in vivo imaging. Taken together, our data demonstrate a novel antimicrobial role for host chemokines against *B. anthracis* that provides unique insight into host defense against inhalational anthrax; these data also support the notion for an innovative approach in treating *B. anthracis* infection as well as infections caused by other spore-forming organisms.

Bacillus anthracis is a gram-positive, spore-forming bacterium that causes the disease anthrax. The infectious *B. anthracis* spore is a dormant, metabolically inactive form of the organism made up of distinct, concentric layers that collectively provide a highly structured casing capable of protecting the spore core from high temperature, UV irradiation, lytic digestion, and numerous reactive agents (31, 59). Spore germination is initiated through receptor-mediated interactions between soluble germinant molecules (typically nutrients such as single amino acids, sugars, or purine nucleosides) and germinant receptors located at the inner membrane of the dormant spore (20, 36). Although the molecular mechanism(s) linking germinant binding to the loss of dormancy is undefined, germinant receptor engagement initiates a cascade of processes, including dipicolinic acid (DPA) release, that promote core rehydration and result in the controlled degradation of the protective spore structures; as germination concludes, metabolic activity resumes, and vegetative outgrowth is initiated (58). Fully virulent *B. anthracis* bacilli generate several virulence factors including

an antiphagocytic, poly-D-glutamic acid capsule encoded by pXO2 (43, 46) and two toxins, lethal toxin and edema toxin, encoded by pXO1 and responsible for disrupting innate and adaptive immune responses (4).

Although recent studies have demonstrated that *B. anthracis* spore germination occurs primarily at initial sites of infection along the respiratory tract (23, 24, 55) in association with macrophages (28, 60), dendritic cells (9, 11), and neutrophils (44, 55), the series of events connecting spore uptake with the appearance of extracellular bacilli remain incompletely defined. It appears that following phagocytosis, spores traffic to phagolysosomes where spore germination occurs (28, 33). While the vast majority of germinating organisms are killed (52, 65), a small subset of germinated spores evades cell-mediated killing mechanisms possibly through early intracellular toxin production (5, 16). Ultimately, vegetative bacilli escape from host phagocytes and establish extracellular infection, leading to toxemia, septicemia, and the subsequent death of the host (18).

Current treatment of inhalational anthrax relies on postexposure prophylaxis with standard antibiotics such as ciprofloxacin or doxycycline for extended periods of time (35). Although antibiotics are effective against the vegetative form of *B. anthracis*, they do not have activity against the dormant spore form of the organism. Thus, the use of antibiotics is limited to established infections that, despite early and vigorous treatment, have high

* Corresponding author. Mailing address: Department of Medicine, Division of Infectious Diseases, University of Virginia Health Sciences System, P.O. Box 800513, Charlottesville, VA 22908. Phone: (434) 924-5216. Fax: (434) 982-3830. E-mail: mah3x@virginia.edu.

[∇] Published ahead of print on 29 January 2009.

morbidity and mortality (37). There are currently no therapeutic agents available that target the spore form of *B. anthracis* and thereby prevent the establishment of infection.

Chemokines are a group of structurally related, low-molecular-mass (8- to 10-kDa) proteins originally defined by their ability to induce directed cell migration in leukocytes (40). Although some chemokines are constitutively expressed and function in homeostatic roles, the majority of chemokines identified thus far are considered to be potent inflammatory mediators induced in response to Toll-like receptor agonists and/or proinflammatory cytokines (42, 51). Three members of the interferon (IFN)-inducible tripeptide motif Glu-Leu-Arg-negative (ELR⁻) CXC chemokines, monokine-induced by IFN- γ (CXCL9), IFN- γ -inducible protein of 10 kDa (CXCL10), and IFN-inducible T-cell-activated chemokine (CXCL11), have been shown to be strongly induced by IFN- γ and together comprise a family of IFN-inducible ELR⁻ CXC chemokines (13, 41, 69).

CXCL9, CXCL10, and CXCL11 are highly homologous proteins that display several common features including a highly positively charged C terminus, similar charge distribution, and amphipathic character (12). CXCL9, CXCL10, and CXCL11 are produced and secreted primarily by monocytes, macrophages, fibroblasts, and epithelial cells upon stimulation with proinflammatory cytokines, especially IFN- γ (19, 39). Each of these chemokines signals through a common G-protein-coupled receptor, CXCR3, and acts primarily in the recruitment of activated CD4⁺ and CD8⁺ T cells, NK cells, and plasmacytoid dendritic cells to sites of inflammation (14, 47). In addition to their roles in leukocyte recruitment, CXCL9, CXCL10, and CXCL11 exert direct antimicrobial effects that are comparable to the effects mediated by cationic antimicrobial peptides, including defensins (12). Antimicrobial activity was subsequently found to extend to a number of chemokines, and the organisms targeted by specific antimicrobial chemokines include the gram-positive bacteria *Staphylococcus aureus*, *Streptococcus mutans*, and *Listeria monocytogenes*; the gram-negative bacteria *Pseudomonas aeruginosa* and *Escherichia coli*; and the fungi *Candida albicans* and *Cryptococcus neoformans* (12, 32, 61, 70).

Based on the above-described information, as well as reports that IFN- γ exerts protective effects against *B. anthracis* challenge in vitro (26) and in vivo (25), we hypothesized that the IFN-inducible CXC chemokines CXCL9, CXCL10, and CXCL11 exert direct antimicrobial effects against *B. anthracis* and thereby promote host defense during inhalational anthrax. CXCL9, CXCL10, and CXCL11 were found to exert direct antimicrobial effects against both the spore and bacillus forms of *B. anthracis*, establishing the first description of direct antimicrobial activity for host chemokines against bacterial spores. In addition, CXC chemokine induction in the lungs of spore-challenged C57BL/6 mice (relatively resistant to inhalational *B. anthracis* infection) was significantly higher than that in the lungs of spore-challenged A/J mice (highly sensitive to infection). The increased level of induction of CXCL9, CXCL10, and CXCL11 was associated with a substantial reduction in detectable spore germination, which is suggestive of a role for CXC chemokine-mediated antimicrobial activity in promoting host defense during the initial stages of *B. anthracis* infection in vivo.

MATERIALS AND METHODS

Bacterial strains, culture conditions, and reagents. *B. anthracis* Sterne strain 7702 (pXO1⁺ pXO2⁻) was used for in vitro experiments; strain 7702 spores were kindly provided by Tod J. Merkel, U.S. Food and Drug Administration (Bethesda, MD). *B. anthracis* bacilli were prepared from the above-mentioned spore stock by streaking diluted spore aliquots onto brain heart infusion (BHI) agar (Remel, Lenexa, KS) plates. A single bacterial colony was subsequently inoculated into 10 ml of BHI broth (BD, Franklin Lakes, NJ) and incubated overnight at 37°C in a shaking incubator (200 rpm). The next day, the bacterial culture was diluted 1:20 in prewarmed BHI broth, and the subculture was incubated at 37°C with shaking until an optical density at 600 nm between 0.6 and 0.65 was achieved. In vivo experiments were performed using *B. anthracis* Sterne strain 34F2 (pXO1⁺ pXO2⁻) carrying the plasmid-based *sspB* promoter-driven *lux* germination reporter, as previously characterized (55). All work involving *B. anthracis* spores and bacilli was performed using biological safety level 2 precautions. Recombinant human CXCL9, CXCL10, CXCL11, CCL2, and CCL5 were purchased from PeproTech (Rocky Hill, NJ). Chemokines were reconstituted at 1 mg/ml in sterile, distilled water stabilized with 0.3% human serum albumin (ZLB Bioplasma AG, Berne, Switzerland) and stored at -80°C.

Chemokine treatment and microscopic visualization. Before treatment, *B. anthracis* spores were heat activated for 30 min in a 70°C water bath to eliminate any germinated organisms; also, since *B. anthracis* bacilli grow in long chains in vitro, bacillus cultures were vortexed before use to limit initial chain length. Spores (0.6×10^5 to 1×10^5 total spores per sample well) or bacilli (2×10^4 to 4×10^4 total bacilli per sample well) were added to high-glucose Dulbecco's modified Eagle's medium (Gibco-Invitrogen, Carlsbad, CA) with 10% fetal bovine serum (HyClone, Logan, UT) containing 48 μ g/ml of individual chemokines or an equal volume of 0.3% human serum albumin (vehicle, untreated control) unless otherwise noted. Aliquots of 100 μ l were plated in triplicate into the wells of a 96-well plate and incubated at 37°C in 5% CO₂. At the same time, an aliquot of the spore or bacillus working stock was diluted and plated onto BHI agar plates for determinations of the initial inoculum. Samples were examined over a 6-h period for spore germination and/or vegetative outgrowth using an Olympus IX51 inverted microscope equipped with a Q-Color3 imaging system (Olympus America, Melville, NY). Camera control and image capture were performed using QCapture Pro 5.1 software (QImaging, Surrey, BC, Canada); images were processed with Adobe (San Jose, CA) Photoshop 7.0. At least eight randomly chosen fields from each treatment group were photographed, and results were confirmed using a second spore preparation and its derived bacilli.

Alamar blue analysis and CFU determination. Active metabolism of *B. anthracis* spores and bacilli with or without chemokine treatment was quantified using the oxidation reduction indicator dye Alamar blue (AbD Serotech, Oxford, United Kingdom), which generates fluorescence in response to the chemical reduction of the treatment medium. At the 4-h time point, Alamar blue was added at a 1:10 dilution to each treatment well including sample blanks lacking *B. anthracis*. The sample plate was then protected from light and incubated for an additional 2 h at 37°C in 5% CO₂. The reduction of Alamar blue as an index of bacterial cell number and proliferation was then assessed by measuring sample well fluorescence at 530-nm excitation and 590-nm emission wavelengths using a Perkin-Elmer Victor³ multilabel plate reader (Perkin-Elmer, Waltham, MA). The addition of Alamar blue at 4 h posttreatment was not found to influence the effects of chemokine treatment or affect subsequent experimental measures.

For CFU determinations, two of the three replicate wells from each treatment group were harvested 6 h posttreatment, and several dilutions were prepared according to predetermined values specific for each treatment (dilution values ranged from no dilution to 1:5,000 and typically resulted in >50 colonies per plate). Sample dilutions were plated in duplicate onto BHI agar plates and incubated overnight at room temperature before colonies were enumerated. In order to differentiate spores from vegetative bacilli in spore treatment groups, sample dilutions were plated with or without heat treatment at 65°C for 30 min, which kills vegetative bacteria.

TEM and silver-enhanced immunogold labeling. *B. anthracis* spores ($\sim 6 \times 10^7$ spores total) or bacilli ($\sim 8 \times 10^6$ bacilli total) were incubated in high-glucose Dulbecco's modified Eagle's medium (permissive to germination) or in water (not permissive to germination) with or without 48 μ g/ml CXCL10 in individual wells of a 24-well plate (500- μ l final volume). At defined time points, untreated and CXCL10-treated samples were harvested and prepared for transmission electron microscopy (TEM) according to standard methods (27). Briefly, experimental samples were fixed with 2.5% glutaraldehyde in 0.1 M phosphate buffer (PB) overnight at 4°C. Samples were subsequently treated with 1% osmium tetroxide in PB for 1 h at room temperature before being dehydrated in a graded ethanol series and embedded in epoxy resin (Epon 812; Electron Microscopy

Sciences, Fort Washington, PA). Ultrathin sections (80 nm) obtained with a Diatorne (Bienne, Switzerland) diamond knife were placed onto 200-mesh nickel grids and contrast stained with lead citrate and uranyl acetate. Sections were examined using a Jeol 1230 transmission electron microscope operated at 80 kV; digital images were captured using an SIA-12 16-megapixel slow-scan charge-coupled device (Scientific Instruments and Applications, Duluth, GA).

Single immunogold labeling with silver enhancement was performed on untreated *B. anthracis* spores at 0 h and on CXCL10-treated spores at 1 h using a preembedding protocol adapted from Aurion (Wageningen, The Netherlands) and described in detail elsewhere (71). Ultrasmall (≤ 1.0 -nm) gold-conjugated F(ab')₂ fragments of goat anti-murine antibody (Ab), acetylated bovine serum albumin, cold-water fish skin gelatin, and R-Gent SE-EM electron microscopy-grade silver enhancement mixture were purchased from Aurion and used according to the manufacturer's instructions. Spore samples were fixed with 4% paraformaldehyde for 30 min at 4°C followed by aldehyde inactivation using 0.1% sodium borohydride in PB. To improve reagent penetration, samples were permeabilized with 0.1% saponin in phosphate-buffered saline (PBS) before incubation in blocking solution (0.2% acetylated bovine serum albumin, 0.1% cold-water fish skin gelatin, 5% normal goat serum in PB). Incubations with primary murine anti-human CXCL10 monoclonal Ab (R&D Systems, Minneapolis, MN) and secondary gold-conjugated F(ab')₂ fragments of goat anti-murine Ab were performed overnight at 4°C in PBS supplemented with 0.2% acetylated bovine serum albumin and 0.1% saponin. Before silver enhancement with the R-Gent SE-EM silver enhancement mixture, postfixation with 2.5% glutaraldehyde was performed. Subsequent sample processing and visualization were performed as described above. Four additional sample groups were prepared in parallel as controls: primary Ab only, secondary Ab only, silver enhancement only, or buffer solution only; gold particles were not visualized in the labeling controls. All electron microscopy studies were performed at the University of Virginia Advanced Microscopy Facility.

In vivo intranasal spore challenge and luminescence detection. In order to analyze spore germination *in vivo*, intranasal *B. anthracis* spore challenge was performed using *B. anthracis* Sterne strain 34F2 carrying a plasmid-based *sspB* promoter-driven *lux* germination reporter (55). Briefly, 6- to 8-week-old female A/J and C57BL/6 mice (Jackson Laboratory, Bar Harbor, ME) were sedated with isoflurane using the XGI-8 gas anesthesia system (Xenogen, Alameda, CA). Thirty microliters of spore suspension ($\sim 1 \times 10^7$ spores total) or sterile water was placed onto the nares of anesthetized mice, and the animals were held upright until the inoculum was inhaled. At 1 h, 6 h, 24 h, and 48 h postchallenge, sham-challenged mice (three to four animals per time point per strain) and *B. anthracis* spore-challenged mice (eight animals per time point per strain) were euthanized by cervical dislocation while sedated. The lungs, livers, and spleens from sham- and spore-challenged mice were harvested and scanned for luminescence using a charge-coupled device within the Xenogen IVIS detection chamber (Xenogen). The emission of photons from sample tissues was quantified using the Living Image 2.5 software package (Xenogen). After luminescence was recorded, the extracted tissues were snap-frozen in liquid nitrogen and stored at -80°C; lung samples were later used for CXC chemokine protein quantification (described below). Animal protocols were reviewed and approved by the Institutional Animal Care and Use Committee of the University of Virginia and the Uniformed Services University.

CXC chemokine protein quantification. Immediately prior to endogenous chemokine quantification, lungs harvested from sham-challenged (three animals per group) and spore-challenged (five animals per group) A/J and C57BL/6 mice were homogenized in 1 ml of cold PBS containing Complete Tab protease inhibitor cocktail (Roche, Basel, Switzerland). The lung samples were homogenized using a Tissuemiser homogenizer (ThermoFisher Scientific, Waltham, MA) and then sonicated three times for 10 s on ice. The lung homogenates were cleared by centrifugation and filtered through a 1.2- μ m Versapor membrane syringe filter (Pall, East Hills, NY).

CXCL9, CXCL10, and CXCL11 protein levels in lung filtrates were determined using the Luminex xMAP technology platform (Luminex, Austin, TX). CXCL9- and CXCL10-specific beads, biotinylated Abs, and protein standards were purchased from Biosource (Nivelles, Belgium) and used according to the manufacturer's instructions. Polyclonal rabbit anti-murine CXCL11 Ab was produced by the immunization of rabbits with recombinant CXCL11 (R&D Systems) as previously described (7). Bead conjugation of the CXCL11 Ab was performed by Upstate (Lake Placid, NY) and was specific in our multiplex assays without cross-reactivity to a panel of cytokines and other CXC and CC chemokine ligands. Biotinylated anti-CXCL11 Ab and CXCL11 protein standards were purchased from R&D Systems. CXC chemokine quantification through multiplex bead array analysis was performed as previously described (64). Briefly, lung homogenate filtrates were incubated in duplicate with a three-bead multiplex

suspension in individual wells of a multiscreen, 96-well filter plate (Millipore, Bedford, MA). A mixture of biotinylated anti-CXCL9, anti-CXCL10, and anti-CXCL11 Abs was added to each well, with the subsequent addition of streptavidin-phycoerythrin (Upstate). The labeling reactions were stopped with the addition of 0.2% paraformaldehyde to the medium, and the sample plate was read using the Bio-Plex 200 suspension array system with Bio-Plex Manager 4.1.1 software (Bio-Rad Laboratories, Hercules, CA). CXC chemokine concentrations were determined from a standard curve assayed at the same time with known amounts of recombinant murine CXCL9, CXCL10, and CXCL11.

Statistical analysis. Statistical analysis and graphing were performed using GraphPad Prism 4.0 software for Windows (GraphPad Software, San Diego, CA). Statistically significant differences were determined using one-way analysis of variance with a Dunnett's post hoc test. Logarithmic (\log_{10}) transformation of bacterial counts (CFU/ml) was performed prior to statistical evaluation. Experimental groups demonstrating statistically significant differences were subsequently analyzed using an unpaired, two-tailed *t* test; a *P* value of <0.05 was considered to be significant. Half-maximal effective concentrations (EC_{50} s) were determined using the sigmoidal dose-response equation of nonlinear regression and are presented as $EC_{50} \pm 95\%$ confidence intervals.

RESULTS

Direct antimicrobial effects of CXCL9, CXCL10, and CXCL11 on *B. anthracis* spores. To investigate possible direct chemokine-mediated antimicrobial effects against *B. anthracis* spores, Sterne strain spores ($pXO1^+ pXO2^-$) were treated with 48 μ g/ml recombinant human CXCL9, CXCL10, or CXCL11 or vehicle alone (untreated control) in tissue culture medium. The concentration chosen for these experiments was based on previous findings that this concentration of chemokine was effective at exerting antimicrobial activity against *E. coli* and *L. monocytogenes* (12). Spore germination and subsequent vegetative cell outgrowth were monitored over a 6-h period using light microscopy (Fig. 1A). Untreated spores began to germinate by 1 h, with subsequent outgrowth such that abundant chains of bacilli were evident by 6 h. In the presence of CXCL9 or CXCL10, spore germination and/or vegetative cell outgrowth was markedly reduced; little to no vegetative bacilli were detected in CXCL10-treated spore samples at 6 h, suggesting a nearly complete absence of germination and primary outgrowth. Although less effective than CXCL9 and CXCL10, CXCL11 also reduced spore germination and/or the outgrowth of vegetative bacilli as determined through light microscopy.

To define the direct effects of CXCL9, CXCL10, and CXCL11 on *B. anthracis* spores quantitatively and determine whether spores or germinated organisms were being affected, two independent methods were used. First, an Alamar blue-based fluorometric assay was used to measure metabolic activity as an index of bacterial cell number and proliferation. Second, CFU determinations were used to measure spore germination, vegetative cell outgrowth, and bacterial viability. In these experiments, monocyte chemotactic protein 1 (CCL2), which has not been found to exert antimicrobial effects, and RANTES (CCL5), which was previously shown to exert antimicrobial effects against *S. aureus* and *C. albicans* (32, 61), were used as controls. These two CC chemokines were chosen since their molecular masses and charges are similar to those of the CXC chemokines tested. As shown in Fig. 1B, levels of Alamar blue reduction were the same for untreated, CCL2-treated, and CCL5-treated spores at 6 h. In addition, CCL2 and CCL5 had no effect on spore germination and/or outgrowth as determined by light microscopy (data not shown). In

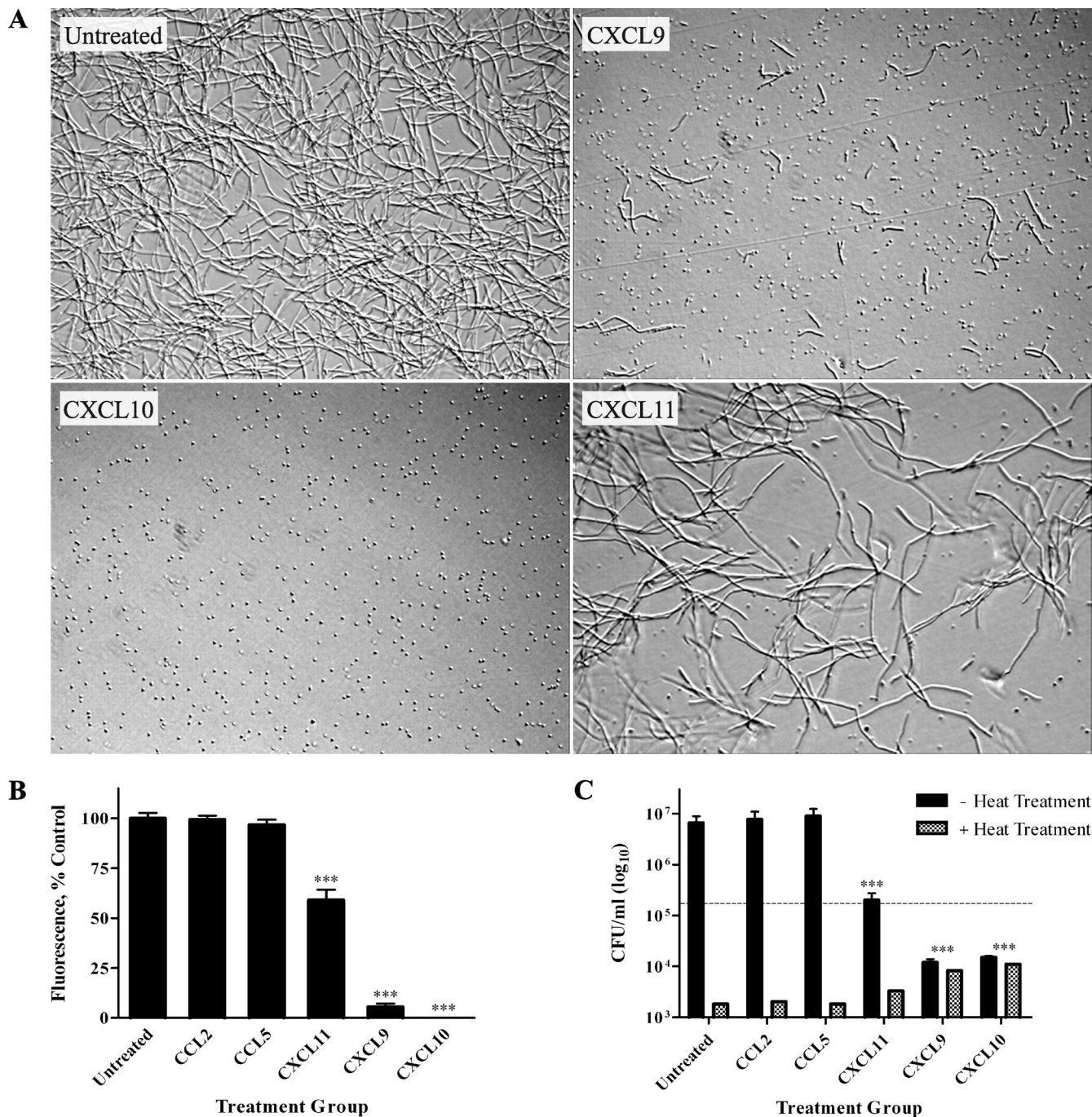


FIG. 1. Direct antimicrobial effects of CXCL9, CXCL10, and CXCL11 against *B. anthracis* spores. (A) *B. anthracis* 7702 spores were treated with vehicle alone (untreated control) or 48 μ g/ml of CXCL9, CXCL10, or CXCL11. All CXC chemokines tested demonstrated antimicrobial activity as assessed by markedly reduced numbers of vegetative bacilli 6 h posttreatment. Representative fields from five independent experiments are shown at a $\times 200$ magnification. (B and C) Alamar blue reduction (B) and CFU determination (C) were determined 6 h posttreatment. In contrast to the untreated and CC chemokine controls, CXCL9, CXCL10, and CXCL11 significantly reduced spore germination and/or vegetative cell outgrowth. CFU determinations were performed with or without heat treatment to differentiate between heat-resistant spores and heat-sensitive bacilli; the dotted line represents the initial spore inoculum. Alamar blue data are expressed as a percentage of untreated control and represent mean values \pm standard errors of the means (SEM) for three independent experiments; CFU data are expressed as CFU/ml (log₁₀ scale) \pm SEM, and a representative data set is shown from three separate experiments. ***, *P* value < 0.001 compared with untreated control.

contrast, spores incubated with CXCL9 or CXCL10 displayed little to no active metabolism (<10% and <1% of the untreated control, respectively; *P* < 0.001), indicating that the chemokine-treated spores consisted of a population of largely

dormant and/or dead organisms. CXCL11 treatment was less effective against *B. anthracis* spores, as reflected by a smaller reduction in metabolic activity (<60% of the untreated control; *P* < 0.001).

CFU determination (Fig. 1C) was performed with or without heat treatment to differentiate between heat-resistant spores and heat-sensitive vegetative bacilli. For experiments with heat treatment, CFU values represent viable, heat-resistant spores; for experiments without heat treatment, CFU values represent both viable spores and vegetative bacilli. By 6 h, the untreated, CCL2-treated, and CCL5-treated spores underwent considerable germination and outgrowth as demonstrated by a loss of heat-resistant CFU and a concomitant increase in heat-sensitive CFU compared to the initial spore inoculum. CXCL9- and CXCL10-treated spore samples demonstrated an approximate 1,000-fold reduction in CFU at 6 h compared to the untreated control. Interestingly, CFU with or without heat treatment were nearly equal, suggesting that there were very few germinated organisms and that the majority of viable organisms were dormant spores. Furthermore, the numbers of heat-resistant CFU (dormant spores) recovered from CXCL9- and CXCL10-treated spore samples were significantly higher than those recovered from untreated samples, yet the CXCL9- and CXCL10-treated sample groups contained approximately 85% fewer viable spores than were in the initial inoculum. These results suggest that CXCL9 and CXCL10 interfere with spore germination and may exert a direct, sporicidal effect on *B. anthracis* spores. CXCL11 treatment did not significantly affect spore germination at the chemokine concentration tested (heat-resistant CFU not significantly greater than those found for the untreated control) but did result in a >10-fold reduction in the subsequent outgrowth of vegetative bacilli. Washing the treatment samples before CFU determination did not affect resultant bacterial CFU, suggesting that chemokine-mediated reductions in viability were irreversible by the time of plating (data not shown).

The direct effects of CXCL9, CXCL10, and CXCL11 were dependent upon chemokine concentration as determined by Alamar blue analysis (Fig. 2A) and CFU determinations (Fig. 2B; data not shown for CXCL9 and CXCL11). Based on Alamar blue analysis, which correlated well with CFU data, the EC_{50} values for CXCL9, CXCL10, and CXCL11 against *B. anthracis* spores were $6.2 \pm 0.2 \mu\text{g/ml}$, $7.9 \pm 0.2 \mu\text{g/ml}$, and $28.2 \pm 1.8 \mu\text{g/ml}$, respectively. Notably, CXCL10 caused a complete inhibition of spore germination and/or vegetative cell outgrowth at a chemokine concentration of $\sim 20 \mu\text{g/ml}$, which was considerably lower than the concentrations of CXCL9 and CXCL11 required to achieve the same effect ($58 \mu\text{g/ml}$ and $72 \mu\text{g/ml}$, respectively). The dissimilar concentration curves among CXCL9, CXCL10, and CXCL11 are likely attributable to differences in the cationic properties of the C-terminal region as well as overall structural characteristics as described elsewhere (12, 70).

CXCL10 affects ungerminated spores and interferes with *B. anthracis* spore germination. The data presented above indicate that CXCL10 exerts direct antimicrobial effects against either *B. anthracis* spores or newly forming bacilli immediately after germination. Since we were unable to distinguish between these two effects using light microscopy, we visualized untreated and CXCL10-treated spores using TEM. *B. anthracis* spores were incubated in the presence or absence of CXCL10 for 6 h before being processed for TEM (Fig. 3A). The untreated spores underwent germination and outgrowth from the initial spore inoculum and were visualized at 6 h as predomi-

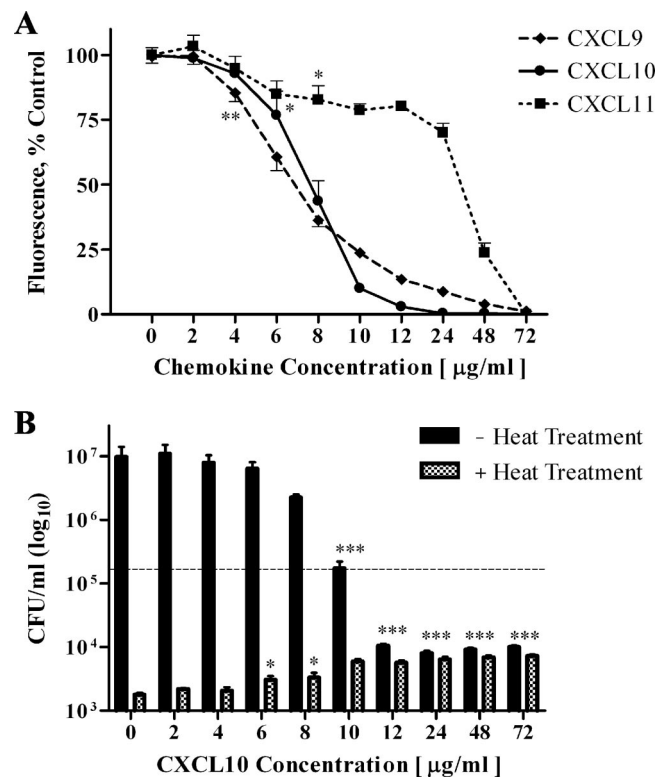


FIG. 2. CXCL9-, CXCL10-, and CXCL11-mediated antimicrobial effects against *B. anthracis* spores are concentration dependent. (A) *B. anthracis* 7702 spores were treated with increasing concentrations of CXCL9, CXCL10, or CXCL11. Alamar blue reduction, as a measure of active metabolism, was determined 6 h posttreatment and used to calculate EC_{50} s ($6.2 \pm 0.2 \mu\text{g/ml}$ for CXCL9, $7.9 \pm 0.2 \mu\text{g/ml}$ for CXCL10, and $28.8 \pm 1.8 \mu\text{g/ml}$ for CXCL11). Alamar blue reduction data are expressed as percentages of the control and represent mean values \pm SEM for two independent experiments. For clarity, only the lowest chemokine concentration demonstrating statistically significant decreases from the untreated control are labeled with asterisks. (B) CFU determination with or without heat treatment of CXCL10-treated *B. anthracis* spores was performed after 6 h of treatment. The direct effects of CXCL10 on spore germination and viability, as described in Results, were dependent on the chemokine concentration; the dotted line represents the initial spore inoculum. CFU data are expressed as CFU/ml (\log_{10} scale) \pm SEM and are a representative data set from two independent experiments. *, P value of <0.05 ; **, P value of <0.01 ; ***, P value of <0.001 (compared with the untreated control).

nately vegetative bacilli. CXCL10-treated spores, however, remained ungerminated as assessed by the lack of cytological changes in spore structure, including cortex degradation, that occur during the germination process in *Bacillus* species (54). These data support the conclusion that CXCL10 interferes with spore germination and demonstrate the ability of CXCL10 to exert direct antimicrobial effects against *B. anthracis* spores.

Since spore germination is a rapid and irreversible process, the inhibitory effects of CXCL10 on *B. anthracis* spore germination likely occur during the initial chemokine interaction with the spore. To determine the initial site(s) of interaction between CXCL10 and *B. anthracis* spores, silver-enhanced immunogold labeling of CXCL10 was performed (Fig. 4). Con-

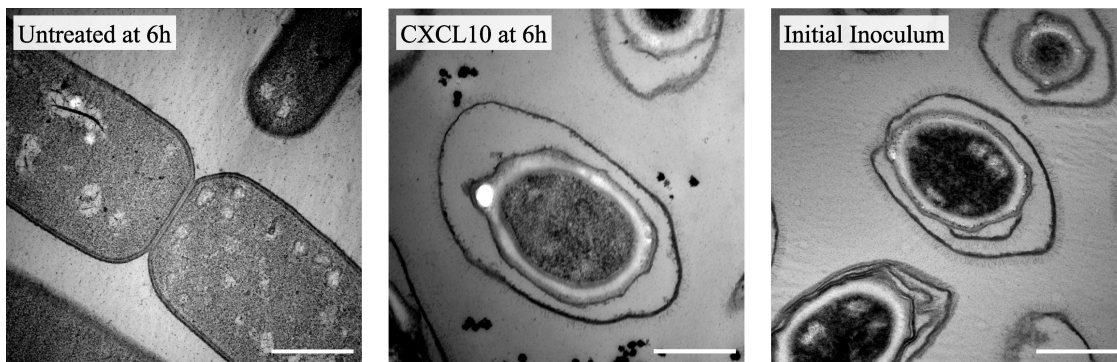


FIG. 3. CXCL10 inhibits *B. anthracis* spore germination prior to cortex degradation. *B. anthracis* 7702 spores with or without 48 µg/ml CXCL10 were visualized 6 h posttreatment using TEM. Whereas untreated spores underwent germination and were visualized as vegetative bacilli, CXCL10-treated spores failed to germinate and closely resembled spores taken from the initial inoculum. Representative fields from two independent experiments are shown at a ×30,000 magnification; the scale bar equals 0.5 µm.

Control spore samples without CXCL10 treatment were processed at 0 h (prior to the initiation of germination) and prepared in the same manner as the CXCL10-treated spores processed for immunogold labeling after 1 h of chemokine treatment in germination-permissive tissue culture medium. Control, ungerminated spores taken from the initial inoculum demonstrated negligible binding of primary anti-CXCL10 Ab and secondary

gold-conjugated F(ab')₂ fragments in the presence of silver enhancement. In the CXCL10-treated spores, silver-enhanced gold particles were found to be associated with the exosporium, spore coat, and spore coat-cortex interface by 1 h. In addition, when CXCL10 treatment was performed in the absence of germinants (i.e., in water), CXCL10 was found to localize to similar spore structures, supporting the conclusion

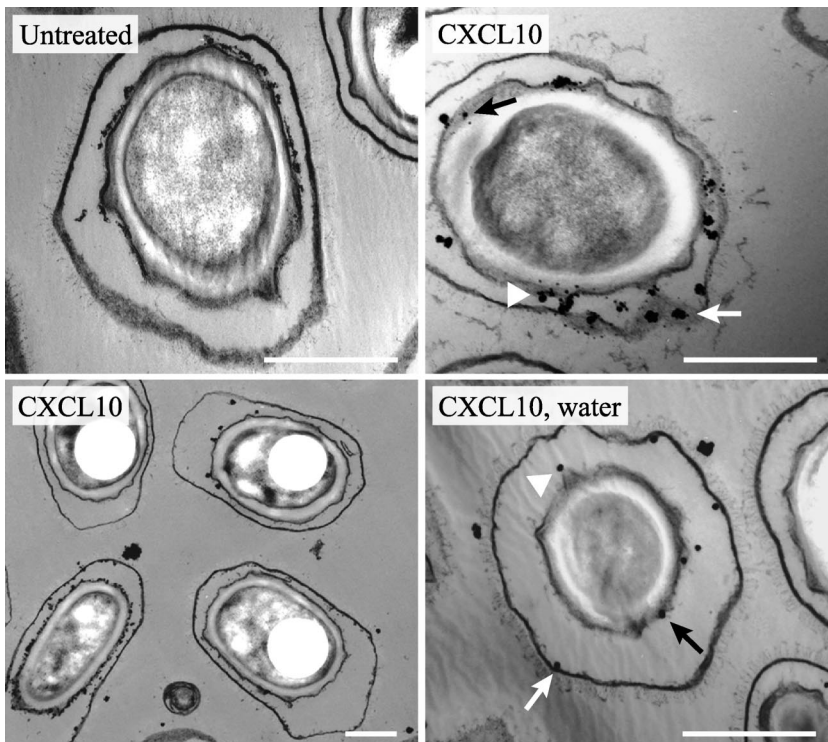


FIG. 4. CXCL10 localizes at spore structures internal to the exosporium. Untreated *B. anthracis* 7702 spores (0 h of treatment) and CXCL10-treated spores (1 h of treatment) were used for immunogold labeling with silver enhancement as described in Materials and Methods. Untreated spores demonstrated negligible binding of labeling reagents. In spores treated with CXCL10, gold particles were found to be associated with the exosporium (white arrow), spore coat (arrowhead), and spore coat-cortex interface (black arrow). A lower-magnification field allowing the visualization of multiple spores immunolabeled for CXCL10 is included. When chemokine treatment was performed in water, conditions not permissive to germination, CXCL10 was found to localize to similar spore structures including the exosporium (white arrow), spore coat (arrowhead), and spore coat-cortex interface (black arrow). Representative fields from 2 independent experiments are shown at a ×30,000 (or ×15,000) magnification; the scale bar equals 0.5 µm.

that CXCL10 acts directly against spores. While the limitations of the technique used for visualization do not exclude the possibility that CXCL10 may be located in the plane of the exosporium, these results strongly suggest that CXCL10 is able to penetrate the outermost spore layers and likely exerts initial antimicrobial effects through interactions with spore components internal to the exosporium.

Direct antimicrobial effects of CXCL9, CXCL10, and CXCL11 on *B. anthracis* vegetative bacilli. To determine whether CXCL9-, CXCL10-, and CXCL11-mediated antimicrobial activity extended to vegetative bacilli, we incubated *B. anthracis* bacilli with 48 $\mu\text{g/ml}$ CXCL9, CXCL10, or CXCL11 or vehicle alone (untreated control) in tissue culture medium. Importantly, since *in vitro* growth of vegetative bacilli occurs in long chains that are difficult to completely disrupt, the initial inoculum consisted primarily of short chains (four to six bacilli) rather than single cells. The outgrowth of vegetative bacilli was monitored over a 6-h period using light microscopy (Fig. 5A). Untreated bacilli underwent significant outgrowth from the initial inoculum by 6 h. In the presence of CXCL9 and CXCL10, vegetative outgrowth was largely absent; although CXCL11-treated bacilli underwent vegetative outgrowth, there were notably fewer vegetative bacilli than the untreated control. The effects of CCL2 and CCL5 on *B. anthracis* bacilli were also tested, and neither CC chemokine inhibited the outgrowth of vegetative bacilli as determined visually (data not shown).

Interestingly, CXCL9- and CXCL10-treated bacilli demonstrated a disruption in bacterial chain integrity in as little as 30 min, with complete chain segmentation by 3 h (Fig. 5A, expanded insets). By 6 h, the majority of bacterial chains had completely separated into individual bacilli. Chain segmentation did not occur in the untreated or CXCL11-treated samples. Bacterial chain disruption similar to that seen for CXCL9- and CXCL10-treated bacilli was also observed when *B. anthracis* bacilli were treated with penicillin G, which acts to disrupt cell wall synthesis and integrity (data not shown). Chain segmentation and subsequent disruption were not observed when vegetative bacilli were treated with ciprofloxacin or gentamicin, which inhibit DNA replication and protein synthesis, respectively. Together, these observations indicate the CXCL9 and CXCL10 may exert antimicrobial effects on *B. anthracis* bacilli by disrupting cell wall and/or cell membrane integrity.

To quantify the direct effects of CXCL9, CXCL10, and CXCL11 on *B. anthracis* bacilli, Alamar blue analysis and CFU determinations were used to measure metabolic activity and viability, respectively. Levels of Alamar blue reduction (Fig. 5B) were similar between untreated, CCL2-treated, and CCL5-treated bacilli at 6 h. Bacilli incubated with CXCL9 or CXCL10, however, displayed markedly reduced levels of active metabolism (<25% and <1% of the untreated control, respectively; $P < 0.001$), which is indicative of a reduction in vegetative cell outgrowth and viability. CXCL11-treated bacilli had significantly impaired outgrowth at 6 h (<70% of the untreated control; $P < 0.001$), consistent with reduced numbers of vegetative bacilli. CFU determinations (Fig. 5C) revealed that by 6 h, the untreated, CCL2-treated, and CCL5-treated vegetative bacilli underwent significant outgrowth from the initial inoculum. CXCL9- and CXCL11-treated bacilli underwent vegetative outgrowth but contained significantly fewer bacilli than did the untreated control at 6 h (CXCL9, >100-fold reduction;

CXCL11, >10-fold reduction). CXCL10 treatment of vegetative bacilli consistently resulted in the complete killing of the initial inoculum, consistent with a potent bactericidal effect. Washing the treatment samples before CFU determination did not affect resultant CFU (data not shown).

CXCL9-, CXCL10-, and CXCL11-mediated antimicrobial effects against *B. anthracis* bacilli were dependent upon chemokine concentrations as determined by Alamar blue analysis (Fig. 6A) and CFU determinations (Fig. 6B; data not shown for CXCL9 and CXCL11). Based on Alamar blue analysis, which matched well with CFU data, the $\text{EC}_{50\text{s}}$ for CXCL9, CXCL10, and CXCL11 against *B. anthracis* bacilli were determined to be $40.2 \pm 1.1 \mu\text{g/ml}$, $4.0 \pm 0.3 \mu\text{g/ml}$, and $72.0 \pm 3.4 \mu\text{g/ml}$, respectively. CXCL10, which is the most potent of the three CXC chemokines examined, demonstrated complete killing of the initial inoculum at concentrations of $\geq 12 \mu\text{g/ml}$. As noted above, the dissimilar effective concentrations among these CXC chemokines likely reflect molecular differences related to cationic charge distribution and structural characteristics (12, 70).

CXCL10 disrupts the cellular integrity of *B. anthracis* bacilli. The antimicrobial effects of CXCL10 against *B. anthracis* bacilli, as described above, suggest that CXCL10 is able to directly mediate the killing of vegetative bacilli. To determine the extent and character of CXCL10-mediated antimicrobial activity, we used TEM to visualize the structural integrity of bacilli incubated for 3 h in the presence or absence of CXCL10 (Fig. 7). Untreated vegetative bacilli were numerous and displayed intact cellular structures complete with membrane septum characteristic of vegetative growth. In contrast, CXCL10-treated bacilli demonstrated a complete loss of cell integrity characterized by extensive cell wall and cell membrane disruption. These observations support the conclusion that CXCL10 exerts bactericidal effects by interfering with the integrity of the bacterial cell wall and/or cell membrane.

In vivo analysis of CXCL9, CXCL10, and CXCL11 levels in lungs of spore-challenged mice. To examine the potential roles of CXCL9, CXCL10, and CXCL11 in promoting host defense against *B. anthracis* infection, we employed a murine model of inhalational anthrax using intranasal spore inoculation (55). The inbred mouse strains chosen for this study were previously shown to be susceptible (A/J) or resistant (C57BL/6) to inhalational infection by the toxigenic, unencapsulated Sterne strain of *B. anthracis* (34, 67). Parallel intranasal spore challenge was performed in A/J mice and C57BL/6 mice; 1 h, 6 h, 24 h, and 48 h after spore challenge, the lungs of sham- and spore-challenged animals were harvested and used to measure CXCL9, CXCL10, and CXCL11 protein levels. Whereas CXCL9, CXCL10, and CXCL11 induction following spore challenge was negligible in the lungs of A/J mice, C57BL/6 mice demonstrated considerable CXC chemokine induction compared to sham-infected controls (Fig. 8); CXCL10 and CXCL11 induction was seen 1 h postchallenge, and CXCL9 was markedly induced by 24 h postchallenge. Compared to infected A/J mice, spore-challenged C57BL/6 mice had significantly higher levels of CXCL9 at 24 h and 48 h ($P < 0.001$) (Fig. 8A) and significantly higher CXCL10 levels at all time points tested ($P < 0.01$ to 0.001) (Fig. 8B). Although CXCL11 levels were low in both inbred strains following spore challenge, the lungs of C57BL/6 animals demonstrated significantly

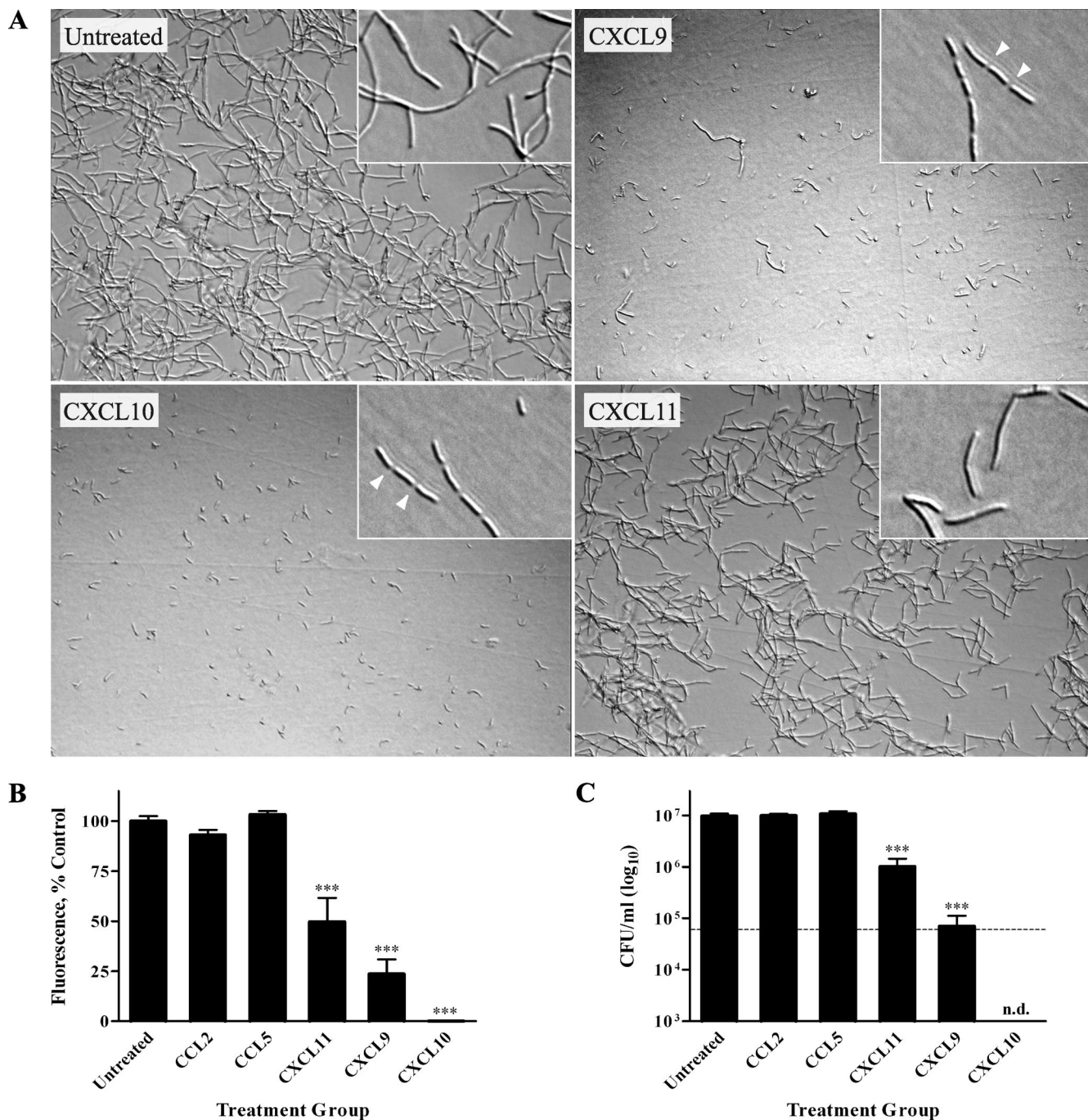


FIG. 5. Direct antimicrobial effects of CXCL9, CXCL10, and CXCL11 against *B. anthracis* bacilli. (A) *B. anthracis* 7702 bacilli were treated with vehicle (untreated control) or 48 μ g/ml of CXCL9, CXCL10, or CXCL11. By 3 h (expanded inserts), CXCL9- and CXCL10-treated bacilli had undergone substantial bacterial chain segmentation (arrowhead) resulting in nearly complete chain disruption by 6 h; chain segmentation and subsequent disruption were not seen in untreated and CXCL11-treated bacillus samples. All three CXC chemokines demonstrated direct antimicrobial effects against *B. anthracis* bacilli as assessed by reduced numbers of vegetative bacilli at 6 h posttreatment. Representative fields from three independent experiments are shown at 6 h (3 h for insets) at a $\times 200$ magnification. (B and C) Alamar blue reduction (B) and CFU determinations (C) were determined 6 h posttreatment. Experimental measures were comparable among untreated, CCL2-treated, and CCL5-treated control groups. CXCL11- and CXCL9-treated bacillus samples demonstrated significantly reduced vegetative cell numbers; CXCL10 treatment resulted in the complete killing (n.d., none detected) of the initial bacillus inoculum (dashed line). Alamar blue data are expressed as a percentage of untreated control and represent mean values \pm SEM for three independent experiments; CFU data are expressed as CFU/ml (log₁₀ scale) \pm SEM, and a representative data set is shown from three separate experiments. ***, *P* value of <0.001 compared with untreated control.

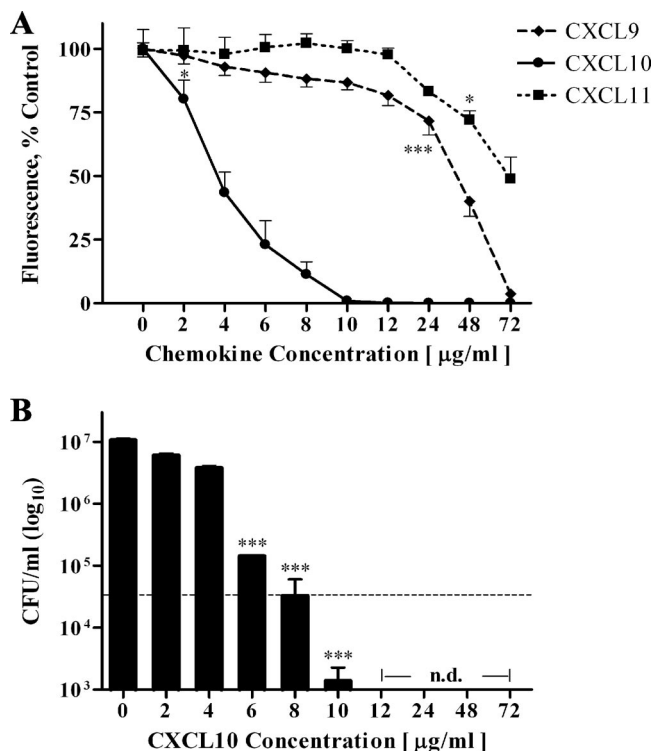


FIG. 6. Direct antimicrobial effects of CXCL9, CXCL10, and CXCL11 against *B. anthracis* bacilli are concentration dependent. (A) *B. anthracis* 7702 vegetative bacilli were treated with increasing concentrations of CXCL9, CXCL10, or CXCL11 for 6 h before Alamar blue reduction was measured. EC₅₀s were determined to be 40.2 ± 1.1 µg/ml, 4.0 ± 0.3 µg/ml, and 72 ± 3.4 µg/ml for CXCL9, CXCL10, and CXCL11, respectively. Alamar blue reduction data are expressed as a percentage of control and represent mean values ± SEM for one to two independent experiments. For clarity, only the lowest chemokine concentrations demonstrating statistically significant decreases from the untreated control are labeled with asterisks. (B) CFU determination of CXCL10-treated vegetative bacilli was performed after 6 h of treatment. CXCL10 concentrations of ≥12 µg/ml resulted in complete killing (n.d., none detected) of the initial inoculum (dashed line). CFU data are expressed as CFU/ml (log₁₀ scale) ± SEM and are a representative data set from two separate experiments. *, *P* value of <0.05; ***, *P* value of <0.001 (compared with untreated control).

higher levels of CXCL11 at 1 h and 24 h (*P* < 0.01 and 0.05, respectively) (Fig. 8C). These data are consistent with a role for CXC chemokine-mediated antimicrobial activity in promoting host defense against inhalational *B. anthracis* infection in vivo.

In vivo analysis of *B. anthracis* spore germination in lungs of spore-challenged mice. The *B. anthracis* Sterne strain spores used in the in vivo intranasal spore challenge studies described above contained a bioluminescent reporter plasmid in which the expression of the *lux* operon signals spore germination (55). This bioluminescent strain allowed us to determine whether the strain-specific differences, as related to the outcome of inhalational *B. anthracis* infection, between A/J and C57BL/6 mice occur before or after spore germination. Using In Vivo Imaging System (IVIS) technology, luminescence was measured in the lungs of sham- and spore-challenged mice at 1 h, 6 h, 24 h, and 48 h postchallenge to determine the extent

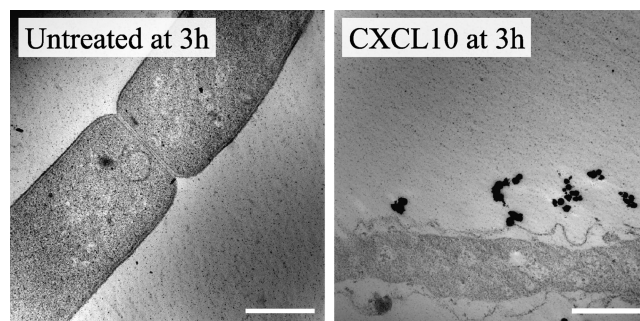


FIG. 7. CXCL10-mediated antimicrobial activity results in the complete loss of *B. anthracis* cell integrity. *B. anthracis* 7702 vegetative bacilli were treated with or without 48 µg/ml CXCL10 for 3 h before being processed for TEM. Untreated bacilli were numerous and displayed a typical cellular structure. Conversely, CXCL10-treated bacilli demonstrated a complete loss of cellular integrity and cell membrane/cell wall structure. Representative fields from two independent experiments are shown at a ×30,000 magnification; the scale bar equals 0.5 µm.

of spore germination (summarized in Fig. 9). Lungs harvested from spore-challenged A/J mice displayed luminescence by 1 h, with increasing levels of luminescence through the 6-h and 24-h time points (Fig. 10A and B); by 48 h, mean luminescent signal intensity in the lungs of spore-challenged A/J mice had begun to decrease. In contrast, lung samples harvested from spore-challenged C57BL/6 mice demonstrated a >90% reduction in spore germination at 1 h compared to spore-challenged A/J mice and were not found to exhibit detectable levels of luminescence at 6 h, 24 h, or 48 h (Fig. 10A and B), indicating that spore germination was absent. Neither inbred mouse strain exhibited luminescence in the spleen or liver following spore challenge, consistent with previous reports that spore germination occurs at initial sites of infection (23, 24, 55). These observations demonstrate that A/J and C57BL/6 mice have differential abilities to prevent spore germination within the lungs, which may act to disrupt the establishment of inhalational *B. anthracis* infection.

DISCUSSION

In the present study, we have established the ability of the IFN-inducible ELR⁻ CXC chemokines CXCL9, CXCL10, and CXCL11 to exert direct antimicrobial effects against *B. anthracis* spores and bacilli in a concentration-dependent manner. The abilities of these host chemokines to inhibit spore germination and reduce spore viability are, to our knowledge, the first description of direct chemokine-mediated antimicrobial effects on bacterial spores and may represent an important mechanism for promoting host defense during the initial stages of inhalational anthrax. In support of this conclusion, we have demonstrated that the induction of CXCL9, CXCL10, and CXCL11 within the lungs of spore-challenged mice was associated with a substantial reduction of spore germination and subsequent disease progression. Taken together, these results open a new avenue of research for examining host chemokines as potential sporicidal/bactericidal agents.

The ability of the IFN-inducible ELR⁻ CXC chemokines to prevent spore germination and directly mediate sporicidal ef-

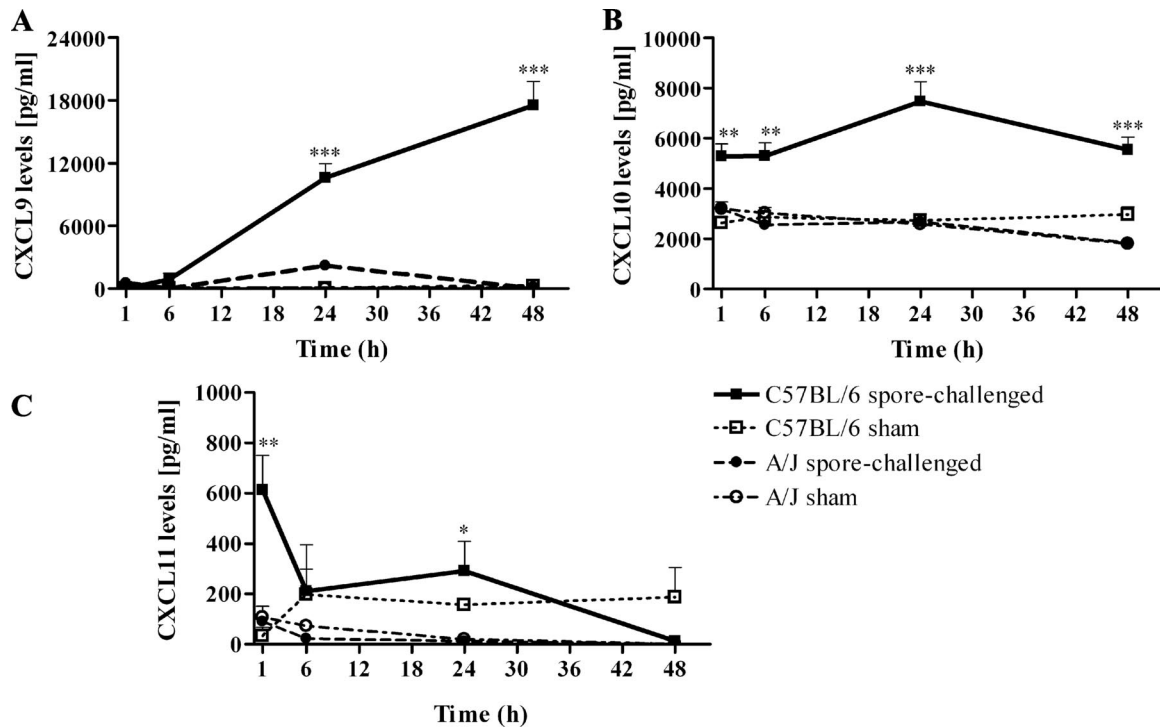


FIG. 8. CXCL9, CXCL10, and CXCL11 responses in the lungs of spore-challenged C57BL/6 and A/J mice. C57BL/6 and A/J mice were challenged intranasally with *B. anthracis* 34F2 spores. Lungs from sham-challenged (three animals per time point per group) and spore-challenged (five animals per time point per group) C57BL/6 and A/J mice were harvested at 1 h, 6 h, 24 h, and 48 h postinfection. CXCL9, CXCL10, and CXCL11 protein levels were determined using Luminex bead array analysis as described in Materials and Methods. (A) CXCL9 levels in the lungs of spore-challenged C57BL/6 mice increased throughout the time course examined and were significantly higher than in the lungs of spore-challenged A/J mice at 24 h and 48 h. (B) CXCL10 levels in the lungs of spore-challenged C57BL/6 mice were induced as early as 1 h and were significantly higher than those found in spore-challenged A/J mice at all time points tested. (C) Spore challenge induced significantly higher CXCL11 levels in the lungs of C57BL/6 mice than in the lungs of A/J mice at 1 h and 24 h. Luminex data are expressed as chemokine concentration (pg/ml) measured in diluted lung homogenate filtrates. Data points represent mean values \pm SEM. *, *P* value of <0.05; **, *P* value of <0.01; ***, *P* value of <0.001.

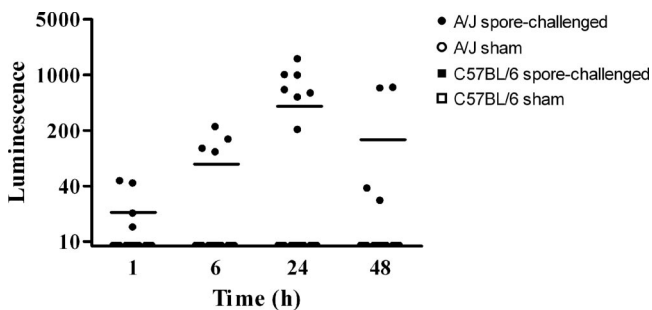


FIG. 9. Relative spore germination in the lungs of sham- and spore-challenged A/J and C57BL/6 mice. A/J and C57BL/6 mice were challenged intranasally with *B. anthracis* 34F2 spores harboring a *lux* reporter construct that is expressed during spore germination. The lungs from sham-challenged (four animals per time point per group) and spore-challenged (eight animals per time point per group) mice were scanned for luminescence at 1 h, 6 h, 24 h, and 48 h postchallenge using IVIS. Spore germination, as measured by luminescence, was observed in the lungs of spore-challenged A/J mice by 1 h, with increasing levels of germination through the 6-h and 24-h time points; by 48 h, the mean luminescent signal intensity in the lungs of spore-challenged A/J mice had begun to decrease. Minimal luminescence (signal intensity of <5) was detected in five of the eight spore-challenged C57BL/6 mice at 1 h postchallenge; no detectable spore germination was observed in the lungs of C57BL/6 mice at 6 h, 24 h, or 48 h as assessed by a lack of luminescent signal. The lungs from all sham-challenged controls were nonluminescent at each time point tested. Data points represent the maximum luminescent signals detected in the lungs of individual mice at the time point indicated; luminescence is reported as photons per second per square centimeter per steradian.

ffects represents novel antimicrobial roles for host chemokines. Defining spore-specific targets and the molecular mechanism(s) of chemokine-mediated antimicrobial activity, however, is complicated by a lack of understanding concerning the mechanistic details of the signaling pathways and molecular interactions involved in spore germination (48). Whereas little data on the inhibition of *B. anthracis* spore germination exist, numerous compounds capable of inhibiting spore germination in *Bacillus* species have been described and include germinant molecule analogs (1), alkyl alcohols (62), ion channel blockers (45), protease inhibitors (8), sulfhydryl reagents (22), and a variety of other compounds (15). While incompletely defined, the mechanisms by which these compounds inhibit spore germination appear to rely on their ability to disrupt germinant receptor engagement and/or the subsequent signaling activities of one or more nutrient receptors (15). Consequently, DPA release (which is essential in triggering cortex hydrolysis during nutrient-mediated germination) is prevented, and spore germination is blocked prior to cortex degradation (15, 58). Notably, the abilities of the above-described compounds to inhibit germination are largely reversible and do not affect spore viability (colony-forming ability), suggesting that subsequent mediators of germination remain functional (15).

Although the effects of CXCL9, CXCL10, and CXCL11 on initial germination events and the possible role of these events

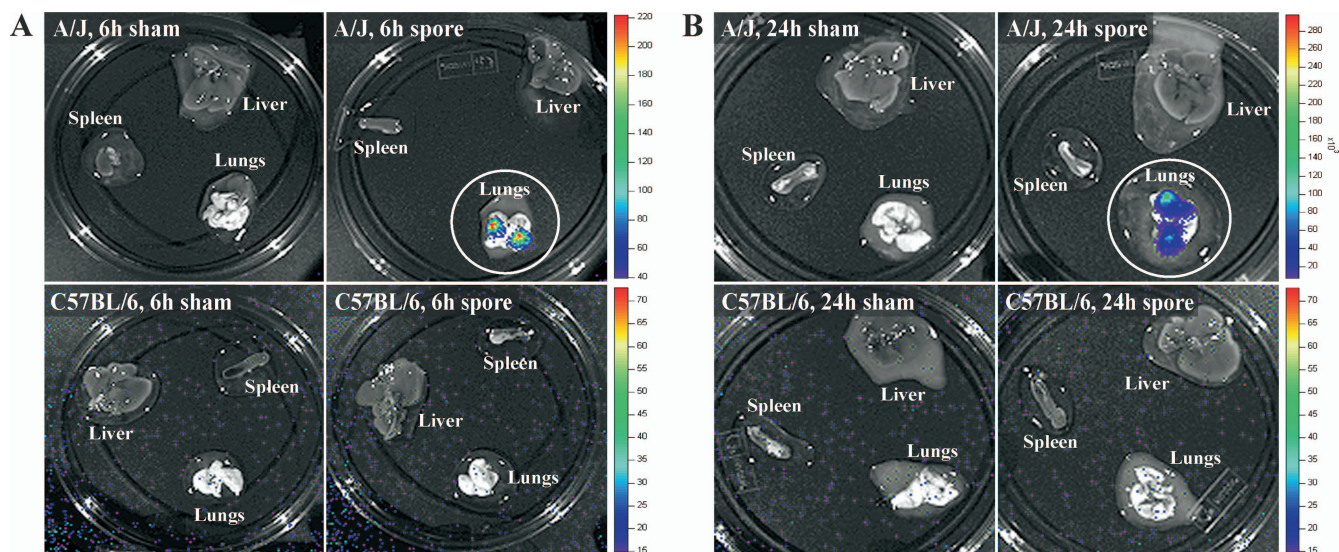


FIG. 10. A/J and C57BL/6 mice differ in their abilities to prevent spore germination within the lungs. A/J and C57BL/6 mice were challenged intranasally with *B. anthracis* 34F2 spores harboring a *lux* reporter construct expressed during spore germination. (A) Lungs, spleen, and liver from sham-challenged (four animals per time point per group) and spore-challenged (eight animals per time point per group) A/J and C57BL/6 mice were scanned for luminescence 6 h postchallenge. Extensive germination, as measured by luminescence signal, was detected in the lungs of spore-challenged A/J mice; the lungs of spore-challenged C57BL/6 mice demonstrated no detectable spore germination at 6 h, and luminescence was absent in all tissues from sham-challenged animals. (B) Tissues harvested from sham- and spore-challenged animals 24 h postchallenge were also scanned for luminescence. Rates of germination in the lungs of spore-challenged A/J mice had increased considerably from 6 h (note that the scale for A/J mice in B is expressed as luminescence values [10^3]). Again, no detectable spore germination was observed in the lungs of C57BL/6 mice, and all sham-challenged tissues were nonluminescent. Neither inbred mouse strain exhibited luminescence in the spleen or liver following spore challenge at any time point examined. Merged photographic and luminescence images are shown for representative animals; luminescence is reported as photons per second per square centimeter per steradian.

in spore susceptibility remain to be determined, TEM visualization of CXCL10-treated *B. anthracis* spores established that the inhibition of spore germination and reduction in spore viability occur prior to spore coat and cortex degradation, demonstrating that CXCL10 directly targets spores and not newly emerging vegetative bacilli. Since ungerminated spores are metabolically inactive, a chemokine-mediated inhibition of macromolecular synthesis as a mechanism for antimicrobial activity is unlikely. These data suggest that CXCL10 exerts its antimicrobial effects by targeting a process inherent, and likely essential, to spore germination and the maintenance of spore viability.

Immunoelectron microscopy demonstrated that CXCL10 associates with the outermost spore layers including the exosporium, spore coat, and spore coat-cortex interface by 1 h, and this localization does not rely on the presence of germinants in the treatment medium. The nonessential nature of the exosporium in spore germination and viability makes it an unlikely target of chemokine-mediated antimicrobial activity. We cannot exclude, however, a possible role for the exosporium, especially since it is the outermost spore layer and is rich in negatively charged carboxylate and phosphate groups (30) that may facilitate initial interactions with the positively charged C-terminal regions of the ELR⁻ CXC chemokines. Although the roles of the spore coat and outer membrane (located at the spore coat-cortex interface) in the process of germination are incompletely defined, studies investigating spore germination in *Bacillus subtilis* and *Bacillus cereus* have identified several components associated with spore germination that localize to these structures and have orthologs in *B. anthracis*. For exam-

ple, cortex-lytic enzymes such as CwlJ, located in the spore coat (3), and SleB, located at the spore coat-cortex interface (49) and inner membrane (10), are responsible for mediating cortex degradation during spore germination. Although the inhibition of these enzymes is consistent with the mechanism of action for several inhibitors of spore germination (2), a recent study suggested that the inhibition of cortex-lytic enzymes is likely an indirect effect and not the primary site of action for these inhibitors (15). Studies of *B. subtilis* and *B. cereus* have also identified a *gerP* operon that encodes proteins thought to be structural components of the spore coat that are important in influencing spore coat permeability and thereby facilitating germinant access to the inner membrane (6). Interestingly, mutational inactivation of the *gerP* locus results in germination defects similar to those seen in CXCL10-treated *B. anthracis* spores, including a block in spore germination prior to cortex hydrolysis, a lower rate of germination, and a reduction in colony-forming ability (6).

It is not currently known whether CXCL10 is able to interact with spore structures in addition to the exosporium, spore coat, and spore coat-cortex interface. Potential CXCL10 localization at the germ cell wall and/or inner membrane may not be identified using immunoelectron microscopy since these sites are likely inaccessible to the relatively large labeling reagents required for visualization. Given the proposed ability of antimicrobial chemokines to interact with bacterial membranes and cell wall components (described below), it is possible that CXCL9, CXCL10, and CXCL11 exert their antimicrobial effects against *B. anthracis* spores by altering the structure of the germ cell wall and/or spore membranes. As a result, the proper

functioning of membrane-associated spore components may be prevented, leading to the irreversible inhibition of spore germination. The possibility that changes in membrane structure and/or membrane protein function can have deleterious effects on spore germination is suggested by tetracaine- and procaine-mediated inhibition of spore germination (45). The mechanisms by which these germination inhibitors act are thought to reflect a disruption in ion efflux and/or DPA release due to increased disordering of the lipid bilayer hydrocarbon interior (15, 73). This type of mechanism would help to explain how chemokine treatment results in the reduction of spore viability; however, it remains to be determined whether the decrease in spore viability upon chemokine treatment occurs via the same mechanism as germination inhibition or whether these effects act through separate, independent mechanisms.

Similar to the abilities of the IFN-inducible ELR⁻ CXC chemokines to mediate direct antimicrobial effects against *B. anthracis* spores, all three CXC chemokines were found to exhibit direct antimicrobial activity against *B. anthracis* bacilli. These data support a growing body of literature demonstrating the ability of host chemokines to target vegetative bacteria through a similar, as-yet-undefined, mechanism. In this regard, chemokines share several biophysical properties, including cationicity and amphipathicity, with antimicrobial peptides that function in innate host defense against infection (72). Furthermore, the C-terminal helical region of antimicrobial chemokines, which is thought to mediate the direct antimicrobial activity of host chemokines, has a structure and amino acid composition similar to those of classical α -helical antimicrobial peptides (72). Due to such similarities, several groups have proposed that chemokines may mediate antimicrobial activity through a similar mechanism in which electrostatic interactions between the cationic host molecule and the anionic microbial surface facilitate interactions resulting in membrane permeabilization and cell lysis (12, 32).

In support of this proposed mechanism of action, CXCL9- and CXCL10-treated vegetative bacilli were found to undergo bacterial chain segmentation with subsequent disruption, consistent with the generation of defects in cell wall and/or cell membrane integrity. These effects on the structural integrity of bacillus chains mimic those seen when vegetative bacilli were treated with penicillin G, which disrupts bacterial cell wall synthesis and results in the loss of bacterial cell integrity (data not shown). In addition, CXCL10-treated bacilli demonstrated a complete loss of cellular integrity as determined through TEM visualization. Although we cannot exclude the possibility that the loss of cellular integrity is a consequence of bactericidal activity rather than the cause, our data do not contradict the current hypothesis that chemokine-mediated antimicrobial activity against vegetative bacteria results from a direct disruption of bacterial membranes and/or cell wall integrity.

The studies described here were performed using the toxigenic, unencapsulated Sterne strain of *B. anthracis* (pXO1⁺ pXO2⁻). Although *B. anthracis* strain differences are thought to be minimal or absent with regard to spores, the presence of the poly-D-glutamic acid capsule may interfere with chemokine-mediated antimicrobial activity against vegetative bacilli. In order to confirm the susceptibility of encapsulated bacilli to CXCL9, CXCL10, and CXCL11, the findings described here will need to be further examined using an encapsulated strain such as the nontoxigenic,

encapsulated Pasteur strain (pXO1⁻ pXO2⁺) or the toxigenic, encapsulated Ames strain (pXO1⁺ pXO2⁺).

In order to begin investigating possible protective roles of chemokine-mediated antimicrobial activity during *B. anthracis* infection *in vivo*, we used a murine model of inhalational anthrax. The lungs of spore-challenged A/J mice, which are susceptible to infection by *B. anthracis* Sterne strain and succumb to inhalational anthrax, did not demonstrate elevated levels of CXCL9, CXCL10, or CXCL11 compared to sham-challenged controls, and extensive spore germination was observed within the lungs at all time points examined, as determined by bioluminescent measurement. In contrast, the lungs of spore-challenged C57BL/6 mice, which are resistant to infection and survive intranasal spore challenge, were found to have significantly higher levels of CXCL9, CXCL10, and CXCL11 than sham-challenged controls; increased chemokine levels were associated with a substantial reduction (1 h) or absence (6 h, 24 h, and 48 h) of detectable spore germination within the lungs of C57BL/6 mice. Although these data support a potential role for chemokine-mediated antimicrobial activity in promoting host defense during infection, they do not differentiate between direct antimicrobial effects and indirect effects resulting from immune cell recruitment to sites of infection. Differentiation of these activities and characterization of potential direct chemokine-mediated effects *in vivo* will require an infection model in which cellular infiltration in response to these chemokines is prevented. While host cell recruitment to CXCL9, CXCL10, and CXCL11 can be disrupted by using mice deficient in the chemokine receptor CXCR3, this lack of cellular infiltration will likely disrupt the positive-feedback loop whereby recruited cells produce factors (e.g., IFN- γ) that promote the induction of these chemokines. Therefore, future experiments will focus on the development of an *in vivo* model in which indirect chemokine-mediated effects are reduced and the overall chemokine production remains comparable to that seen during infection. When discussing the *in vivo* data presented in this paper, it is also important to recognize known differences among the mouse strains used as well as differences between *in vitro* and *in vivo* chemokine concentrations.

Previous studies have attributed differences in susceptibility to *B. anthracis* infection among inbred murine strains to a deficiency in complement. Specifically, host resistance to Sterne strain infection has been shown to be associated with the host's ability to produce complement component 5 (C5), and complement depletion in normally resistant mice renders them highly susceptible to inhalational Sterne strain infection (29, 66). Although a direct role for C5 in controlling Sterne strain infection has not been determined, several explanations have been proposed, including increased phagocytic killing and the promotion of immune cell infiltration to sites of infection (66). In the present context, the latter explanation is particularly interesting since a defect in C5a, a chemotactic cleavage product of C5, would likely disrupt host cell recruitment during inhalational *B. anthracis* infection and may prevent the induction of the interferon-inducible ELR⁻ CXC chemokines. Along these lines, C5a neutralization has been shown to significantly reduce CXC and CC chemokine production by alveolar macrophages *in vivo* (17). Similarly, C5 depletion has been found to inhibit production of IFN- γ , a potent inducer of the ELR⁻ CXC chemokines, and prevent the induction of proin-

flammatory cytokines and chemokines during experimental sepsis (21, 63).

All antimicrobial chemokines characterized to date, including those presented here, mediate direct antimicrobial effects within a concentration range that is higher than that required for inducing directed cell migration (12, 32, 61). In the present study, the concentrations of CXCL9, CXCL10, and CXCL11 measured from the lungs of spore-challenged animals were lower than the concentrations used in the *in vitro* studies. The notion that direct chemokine-mediated antimicrobial activity is likely to be relevant during infection is supported by several published studies, including that (i) the stimulation of peripheral blood mononuclear cells with IFN- γ induces the production of CXCL9 and CXCL10 to levels calculated to be capable of exerting direct antimicrobial effects against *E. coli* (12); (ii) supernatants from IFN- γ /tumor necrosis factor alpha-stimulated normal human bronchial epithelial cells demonstrate IFN-inducible ELR⁻ CXC chemokine concentrations of several hundred nanograms per milliliter, with CXCL10 levels approaching 1 μ g/ml (56); and (iii) markedly elevated concentrations of CXCL9 (>170 ng/ml) and CXCL10 (>400 ng/ml) have been shown to be present in the plasma of patients with melioidosis and correlate with the severity and outcome of infection (38). While the above-described studies support that the ELR⁻ CXC chemokines are part of the innate immune response to bacterial infections, these concentrations are lower than the effective *in vitro* concentrations used in this study. Local chemokine concentrations at sites of infection, however, are likely higher than those measured in whole-tissue filtrates or cell culture supernatants and may reach levels sufficient for exerting antimicrobial effects through the individual or additive effects of these CXC chemokines.

Further support for a potential role of direct chemokine-mediated antimicrobial activity during infection comes from studies examining the effector functions of antimicrobial peptides, including defensins. The α -, β -, and θ -defensins exhibit antimicrobial activity *in vitro* at concentrations in the microgram-per-milliliter range (57), much like the direct chemokine-mediated antimicrobial activity described in the present study. Despite relatively high effective concentrations *in vitro*, defensins have been shown to play a critical role in innate host defense against bacterial challenge. Several transgenic mouse studies have provided evidence for defensin-mediated antibacterial effector functions *in vivo* and include (i) delayed clearance of *Haemophilus influenzae* from the lungs of mice deficient in mouse β -defensin-1 (50), (ii) reductions in bacterial burden and increased survival rates following challenge with *Salmonella enterica* serovar Typhimurium in mice expressing human defensin 5 (53), and (iii) increased virulence of *E. coli* in mice deficient in Paneth cell α -defensins (68). Taken together, these *in vivo* studies provide evidence for a physiological function of defensins in promoting host defense and suggest that the chemokine concentrations presented in the current study are not so high as to preclude them from exerting antimicrobial activity *in vivo*.

Given ongoing concerns about the threat posed by weaponized *B. anthracis* spores and the inability of current treatment options to prevent the establishment of anthrax, novel therapeutic strategies capable of effectively targeting the early stages of *B. anthracis* infection are required. The ability of

CXCL9, CXCL10, and CXCL11 to affect both *B. anthracis* spores and bacilli establishes a novel antimicrobial effect of these chemokines. Also, their induction by the administration of exogenous IFN- γ may offer an effective way of augmenting the production of protective CXCL9, CXCL10, and CXCL11 levels in the host lungs. By understanding the mechanism(s) by which these chemokines target *B. anthracis* spores and vegetative bacilli and their ability to promote host defense during infection, it is likely that innovative therapeutic strategies can be devised for effectively treating and/or preventing inhalational *B. anthracis* infection. In addition, these findings will likely have a therapeutic impact on infections caused by a range of pathogenic and potentially multidrug-resistant bacteria including other spore-forming organisms such as *Clostridium difficile*.

ACKNOWLEDGMENTS

This work was supported by the Virginia Commonwealth Health Research Board (M.A.H.) and by National Institutes of Health National Institute of Allergy and Infectious Diseases grant U54 AI057168 and Mid-Atlantic Regional Center of Excellence in Biodefense and Emerging Infectious Diseases (M.A.H. and A.D.O.). Support was also provided by National Institutes of Health grant T32 AI055432-05, Biodefense Research Training and Career Development (M.A.C.).

We thank Erik Hewlett and the members of his laboratory for helpful discussions and advice. We also thank Jan Redick for her assistance with transmission electron microscopy analysis and immunogold labeling procedures.

We have declared that no conflict of interest exists.

REFERENCES

- Akoachere, M., R. C. Squires, A. M. Nour, J. Brojatsch, and E. Abel-Santos. 2007. Identification of an *in vivo* inhibitor of *Bacillus anthracis* spore germination. *J. Biol. Chem.* **282**:12112–12118.
- Alvarez, Z., and E. Abel-Santos. 2007. Potential use of inhibitors of bacteria germination in the prophylactic treatment of anthrax and *Clostridium difficile*-associated disease. *Expert Rev. Anti-Infect. Ther.* **5**:783–792.
- Bagyan, I., and P. Setlow. 2002. Localization of the cortex lytic enzyme CwlJ in spores of *Bacillus subtilis*. *J. Bacteriol.* **184**:1219–1224.
- Baldari, C. T., F. Tonello, S. R. Pacani, and C. Montecucco. 2006. Anthrax toxins: a paradigm of bacterial immune suppression. *Trends Immunol.* **27**:434–440.
- Banks, D. J., M. Barnajian, F. J. Maldonado-Arocho, A. M. Sanchez, and K. A. Bradlet. 2005. Anthrax toxin receptor 2 mediates *Bacillus anthracis* killing of macrophages following spore challenge. *Cell. Microbiol.* **7**:1173–1185.
- Behravan, J., H. Chirakkal, A. Masson, and A. Moir. 2000. Mutations in the *gerP* locus of *Bacillus subtilis* and *Bacillus cereus* affect access of germinants to their targets in spores. *J. Bacteriol.* **182**:1987–1994.
- Belperio, J. A., M. P. Keane, M. D. Burdick, J. P. Lynch III, Y. Y. Xue, K. Li, D. J. Ross, and R. M. Strieter. 2002. Critical role for CXCR3 chemokine biology in the pathogenesis of bronchiolitis obliterans syndrome. *J. Immunol.* **169**:1037–1049.
- Boschwitz, H., Y. Milner, A. Keynan, H. O. Halvorson, and W. Troll. 1983. Effect of inhibitors of trypsin-like proteolytic enzymes *Bacillus cereus* T spore germination. *J. Bacteriol.* **153**:700–708.
- Brittingham, K. C., G. Ruthel, R. G. Panchal, C. L. Fuller, W. J. Ribot, T. A. Hoover, H. A. Young, A. O. Anderson, and S. Bavari. 2005. Dendritic cells endocytose *Bacillus anthracis* spores: implications for anthrax pathogenesis. *J. Immunol.* **174**:5545–5552.
- Chirakkal, H., M. O'Rourke, A. Atrih, S. J. Foster, and A. Moir. 2002. Analysis of spore cortex lytic enzymes and related proteins in *Bacillus subtilis* endospore germination. *Microbiology* **148**:2383–2392.
- Cleret, A., A. Quesnel-Hellmann, A. Vallon-Eberhard, B. Verrier, S. Jung, D. Vidal, J. Mathieu, and J. N. Tournier. 2007. Lung dendritic cells rapidly mediate anthrax spore entry through the pulmonary route. *J. Immunol.* **178**:7994–8001.
- Cole, A. M., T. Ganz, A. M. Liese, M. D. Burdick, L. Liu, and R. M. Strieter. 2001. IFN-inducible ELR⁻ CXC chemokines display defensin-like antimicrobial activity. *J. Immunol.* **167**:623–627.
- Cole, K. E., C. A. Strick, T. J. Paradis, K. T. Ogborne, M. Loetscher, R. P. Gladue, W. Lin, J. G. Boyd, B. Moser, D. E. Wood, B. G. Sahagan, and K.

- Neote. 1998. Interferon-inducible T cell alpha chemoattractant (I-TAC): a novel non-ELR CXC chemokine with potent activity on activated T cells through selective high affinity binding to CXCR3. *J. Exp. Med.* **187**:2009–2021.
14. Colonna, M., G. Trinchieri, and Y. J. Liu. 2004. Plasmacytoid dendritic cells in immunity. *Nat. Immunol.* **5**:1219–1226.
 15. Cortezzo, D. E., B. Setlow, and P. Setlow. 2004. Analysis of the action of compounds that inhibit the germination of spores of *Bacillus* species. *J. Appl. Microbiol.* **96**:725–741.
 16. Cote, C. K., T. L. DiMezzo, D. J. Banks, B. France, K. A. Bradley, and S. L. Welkos. 2008. Early interactions between fully virulent *Bacillus anthracis* and macrophages that influence the balance between spore clearance and development of a lethal infection. *Microbes Infect.* **10**:613–619.
 17. Czermak, B. J., V. Sarma, N. M. Bless, H. Schmal, H. P. Friedl, and P. A. Ward. 1999. In vitro and in vivo dependency of chemokine generation on C5a and TNF- α . *J. Immunol.* **162**:2321–2325.
 18. Dixon, T. C., M. Meselson, J. Guillemin, and P. C. Hanna. 1999. Anthrax. *N. Engl. J. Med.* **341**:815–826.
 19. Farber, J. M. 1997. Mig and IP-10: CXC chemokines that target lymphocytes. *J. Leukoc. Biol.* **61**:246–257.
 20. Fisher, N., and P. Hanna. 2005. Characterization of *Bacillus anthracis* germinant receptors in vitro. *J. Bacteriol.* **187**:8055–8062.
 21. Flierl, M. A., D. Rittirsch, B. A. Nadeau, D. E. Day, F. S. Zetoune, J. V. Sarma, M. S. Huber-Lang, and P. A. Ward. 2008. Functions of the complement components C3 and C5 during sepsis. *FASEB J.* **22**:3483–3490.
 22. Foster, S. J., and K. Johnstone. 1986. The use of inhibitors to identify early events during *Bacillus megaterium* KM spore germination. *Biochem. J.* **237**:865–870.
 23. Glomski, I. J., A. Piris-Gimenez, M. Huerre, M. Mock, and P. L. Goossens. 2007. Primary involvement of pharynx and Peyer's patch in inhalational and intestinal anthrax. *PLoS Pathog.* **3**:e76.
 24. Glomski, I. J., F. Dumetz, G. Jouvion, M. R. Huerre, M. Mock, and P. L. Goossens. 2008. Inhaled non-capsulated *Bacillus anthracis* in A/J mice: nasopharynx and alveolar space as dual portals of entry, delayed dissemination, and specific organ targeting. *Microbes Infect.* **10**:1398–1404.
 25. Glomski, I. J., J. P. Corre, M. Mock, and P. L. Goossens. 2007. IFN-gamma-producing CD4 T lymphocytes mediate spore-induced immunity to capsulated *Bacillus anthracis*. *J. Immunol.* **178**:2646–2650.
 26. Gold, J. A., Y. Hoshino, S. Hoshino, M. B. Jones, A. Nolan, and M. D. Weiden. 2004. Exogenous gamma and alpha/beta interferon rescues human macrophages from cell death induced by *Bacillus anthracis*. *Infect. Immun.* **72**:1291–1297.
 27. Graham, L., and J. M. Orenstein. 2007. Processing tissue and cells for transmission electron microscopy in diagnostic pathology and research. *Nat. Protoc.* **2**:2439–2450.
 28. Guidi-Rontani, C., M. Weber-Levy, E. Labruyere, and M. Mock. 1999. Germination of *Bacillus anthracis* spores within alveolar macrophages. *Mol. Microbiol.* **31**:9–17.
 29. Harvill, E. T., G. Lee, V. K. Grippe, and T. J. Merkel. 2005. Complement depletion renders C57BL/6 mice sensitive to the *Bacillus anthracis* Sterne strain. *Infect. Immun.* **73**:4420–4422.
 30. He, L. M., and B. M. Tebo. 1998. Surface charge properties of and Cu(II) adsorption by spores of the marine *Bacillus* sp. strain SG-1. *Appl. Environ. Microbiol.* **64**:1123–1129.
 31. Henriques, A. O., and C. P. Moran. 2007. Structure, assembly, and function of the spore surface layers. *Annu. Rev. Microbiol.* **61**:555–588.
 32. Hieshima, K., H. Ohtani, M. Shibano, D. Izawa, T. Nakayama, Y. Kawasaki, F. Shiba, M. Shiota, F. Katou, T. Saito, and O. Yoshie. 2003. CCL28 has dual roles in mucosal immunity as a chemokine with broad-spectrum antimicrobial activity. *J. Immunol.* **170**:1452–1461.
 33. Hu, H., Q. Sa, T. M. Koehler, A. I. Aronson, and D. Zhou. 2006. Inactivation of *Bacillus anthracis* spores in murine primary macrophages. *Cell. Microbiol.* **8**:1634–1642.
 34. Hughes, M. A., C. S. Green, L. Lowchijj, G. M. Lee, V. K. Grippe, M. F. Smith, Jr., L. Y. Huang, E. T. Harvill, and T. Merkel. 2005. MyD88-dependent signaling contributes to protection following *Bacillus anthracis* spore challenge of mice: implications for Toll-like receptor signaling. *Infect. Immun.* **73**:7535–7540.
 35. Inglesby, T. V., D. A. Henderson, J. G. Bartlett, M. S. Ascher, E. Eitzen, A. M. Friedlander, J. Hauer, J. McDade, M. T. Osterholm, T. O'Toole, G. Parker, T. M. Perl, P. K. Russell, and K. Tonat. 1999. Anthrax as a biological weapon: medical and public health management. *JAMA* **281**:1735–1745.
 36. Ireland, J. W., and P. C. Hanna. 2002. Amino acid- and purine ribonucleoside-induced germination of *Bacillus anthracis* Δ Sterne endospores: *gerS* mediates responses to aromatic ring structures. *J. Bacteriol.* **184**:1296–1303.
 37. Jernigan, J. A., D. S. Stephens, D. A. Ashford, C. Omenaca, M. S. Topiel, M. Galbraith, M. Tapper, T. L. Fisk, S. Zaki, T. Popovic, R. F. Meyer, C. P. Quinn, S. A. Harper, S. K. Fridkin, J. J. Sejvar, C. W. Shepard, M. McConnell, J. Guarner, W. J. Shieh, J. M. Malecki, J. L. Gerberding, J. M. Hughes, and B. A. Perkins. 2001. Bioterrorism-related inhalational anthrax: the first 10 cases reported in the United States. *Emerg. Infect. Dis.* **7**:933–944.
 38. Lauw, F. N., A. J. Simpson, J. M. Prins, S. J. van Deventer, W. Chaowagul, N. J. White, and T. van der Poll. 2000. The CXC chemokines gamma interferon (IFN- γ)-inducible protein 10 and monokine induced by IFN- γ are released during severe melioidosis. *Infect. Immun.* **68**:3888–3893.
 39. Luster, A. D., and J. V. Ravetch. 1987. Biochemical characterization of a gamma interferon-inducible cytokine (IP-10). *J. Exp. Med.* **166**:1084–1097.
 40. Luster, A. D. 1998. Chemokines—chemotactic cytokines that mediate inflammation. *N. Engl. J. Med.* **338**:436–445.
 41. Luster, A. D., J. C. Unkeless, and J. V. Ravetch. 1985. Gamma-interferon transcriptionally regulates an early-response gene containing homology to platelet proteins. *Nature* **315**:672–676.
 42. Luster, A. D. 2002. The role of chemokines in linking innate and adaptive immunity. *Curr. Opin. Immunol.* **14**:129–135.
 43. Makino, S., I. Uchida, N. Terakado, C. Sasakawa, and M. Yoshikawa. 1989. Molecular characterization and protein analysis of the cap region, which is essential for encapsulation in *Bacillus anthracis*. *J. Bacteriol.* **171**:722–730.
 44. Mayer-Scholl, A., R. Hurwitz, V. Brinkmann, M. Schmid, P. Jungblut, Y. Weinrauch, and A. Zychlinsky. 2005. Human neutrophils kill *Bacillus anthracis*. *PLoS Pathog.* **1**:e23.
 45. Mitchell, C., J. F. Skomurski, and J. C. Vary. 1986. Effect of ion-channel blockers on germination of *Bacillus megaterium* spores. *FEMS Microbiol. Lett.* **34**:211–214.
 46. Mock, M., and A. Fouet. 2001. Anthrax. *Annu. Rev. Microbiol.* **55**:647–671.
 47. Mohan, K., E. Cordeiro, M. Vaci, C. McMaster, and T. B. Issekutz. 2005. CXCR3 is required for migration to dermal inflammation by normal and in vivo activated T cells: differential requirements by CD4 and CD8 memory subsets. *Eur. J. Immunol.* **35**:1702–1711.
 48. Moir, A. 2006. How do spores germinate? *J. Appl. Microbiol.* **101**:526–530.
 49. Moriyama, R., H. Fukuoka, S. Miyata, S. Kudoh, A. Hattori, S. Kozuka, Y. Yasuda, K. Tochikubo, and S. Makino. 1999. Expression of a germination-specific amidase, SleB, of bacilli in the forespore compartment of sporulating cells and its localization on the exterior side of the cortex in dormant spores. *J. Bacteriol.* **181**:2373–2378.
 50. Moser, C., D. J. Weiner, E. Lysenko, R. Bals, J. N. Weiser, and J. M. Wilson. 2002. Beta-defensin 1 contributes to pulmonary innate immunity in mice. *Infect. Immun.* **70**:3068–3072.
 51. Rossi, D., and A. Zlotnik. 2000. The biology of chemokines and their receptors. *Annu. Rev. Immunol.* **18**:217–242.
 52. Ruthel, G., W. J. Ribot, S. Bavari, and T. A. Hoover. 2004. Time-lapse confocal imaging of development of *Bacillus anthracis* in macrophages. *J. Infect. Dis.* **189**:1313–1316.
 53. Salzman, N. H., D. Ghosh, K. M. Huttner, Y. Paterson, and C. L. Bevins. 2003. Protection against enteric salmonellosis in transgenic mice expressing a human intestinal defensin. *Nature* **422**:522–526.
 54. Santo, L. Y., and R. H. Doi. 1974. Ultrastructural analysis during germination and outgrowth of *Bacillus subtilis* spores. *J. Bacteriol.* **120**:475–481.
 55. Sanz, P., L. D. Teel, A. Farhang, H. M. Carvalho, S. C. Darnell, and A. D. O'Brien. 2008. Detection of *Bacillus anthracis* spore germination in vivo by bioluminescence imaging. *Infect. Immun.* **76**:1036–1047.
 56. Sauty, A., M. Dziejman, R. A. Taha, A. S. Iarossi, K. Neote, E. A. Garcia-Zepeda, Q. Hamia, and A. D. Luster. 1999. The T cell-specific CXC chemokines IP-10, Mig, and I-TAC are expressed by activated human bronchial epithelial cell. *J. Immunol.* **162**:3549–3558.
 57. Selsted, M. E., and A. J. Ouellette. 2005. Mammalian defensins in the antimicrobial immune response. *Nat. Immunol.* **6**:551–557.
 58. Setlow, P. 2003. Spore germination. *Curr. Opin. Microbiol.* **6**:550–560.
 59. Setlow, P. 2006. Spores of *Bacillus subtilis*: their resistance to and killing by radiation, heat, and chemicals. *J. Appl. Microbiol.* **101**:514–525.
 60. Shafa, F., B. J. Moberly, and P. Gerhardt. 1966. Cytological features of anthrax spores phagocytized in vitro by rabbit alveolar macrophages. *J. Infect. Dis.* **116**:401–413.
 61. Tang, Y. Q., M. R. Yeaman, and M. E. Selsted. 2002. Antimicrobial peptides from human platelets. *Infect. Immun.* **70**:6524–6533.
 62. Trujillo, R., and N. Laible. 1970. Reversible inhibition of spore germination by alcohols. *Appl. Microbiol.* **20**:620–623.
 63. Tsuji, R. F., G. P. Geba, Y. Wang, K. Kawamoto, L. A. Matis, and P. W. Askenase. 1997. Required early complement activation in contact sensitivity with generation of local C5-dependent chemotactic activity, and late T cell interferon gamma: a possible initiating role of B cells. *J. Exp. Med.* **186**:1015–1026.
 64. Weber, J., V. K. Sondak, R. Scotland, R. Phillip, F. Wang, V. Rubio, T. B. Stuge, S. G. Groshen, C. Gee, G. G. Jeffery, S. Sian, and P. P. Lee. 2003. Granulocyte-macrophage-colony-stimulating factor added to a multipeptide vaccine for resected stage II melanoma. *Cancer* **97**:186–200.
 65. Welkos, S., A. Friedlander, S. Weeks, S. Little, and I. Mendelson. 2002. In vitro characterization of the phagocytosis and fate of anthrax spores in macrophages and the effects of anti-PA antibody. *J. Med. Microbiol.* **51**:821–831.
 66. Welkos, S. L., and A. M. Friedlander. 1988. Pathogenesis and genetic control of resistance to the Sterne strain of *Bacillus anthracis*. *Microb. Pathog.* **4**:53–69.

67. **Welkos, S. L., T. J. Keener, and P. H. Gibbs.** 1986. Differences in susceptibility of inbred mice to *Bacillus anthracis*. *Infect. Immun.* **51**:795–800.
68. **Wilson, C. L., A. J. Ouellette, D. P. Satchell, T. Ayabe, Y. S. Lopez-Boado, J. L. Stratman, S. J. Hultgren, L. M. Matrisian, and W. C. Parks.** 1999. Regulation of intestinal alpha-defensin activation by the metalloproteinase matrilysin in innate host defense. *Science* **286**:113–117.
69. **Wright, T. M., and J. M. Farber.** 1991. 5' regulatory region of a novel cytokine gene mediates selective activation by interferon gamma. *J. Exp. Med.* **173**:417–422.
70. **Yang, D., Q. Chen, D. M. Hoover, P. Stanley, K. D. Tucker, J. Lubkowski, and J. J. Oppenheim.** 2003. Many chemokines including CCL20/MIP-3alpha display antimicrobial activity. *J. Leukoc. Biol.* **74**:448–455.
71. **Yi, H., J. M. Leunissen, G. M. Shi, C. A. Gutekunst, and S. Hersch.** 2001. A novel procedure for pre-embedding double immunogold-silver labeling at the ultrastructural level. *J. Histochem. Cytochem.* **49**:279–283.
72. **Yount, N. Y., A. S. Bayer, Y. Q. Xiong, and M. R. Yeaman.** 2006. Advances in antimicrobial peptide immunobiology. *Biopolymers* **84**:435–458.
73. **Yun, I., E. S. Cho, H. O. Jang, U. K. Kim, C. H. Choi, I. K. Chung, I. S. Kim, and W. W. Gibson.** 2002. Amphiphilic effects of local anesthetics on rotational mobility in neuronal and model membranes. *Biochim. Biophys. Acta* **1564**:123–132.

Editor: S. R. Blanke